Possibility of breakdown of overdamped and narrowing limits in low-frequency Raman spectra: Phenomenological band-shape analysis using the multiple-random-telegraph model

Yuko Amo
Research Center for Advanced Science and Technology, University of Tokyo, 4-6-1 Komaba, Meguro-ku, Tokyo 153-0041, Japan

Yasunori Tominaga
Graduate School of Humanities and Sciences, Ochanomizu University, Otsuka, Bunkyo-ku, Tokyo 112-8610, Japan
(Received 29 December 1998)

Depolarized low-frequency Raman spectra of liquid water and heavy water are investigated from 266 K to 356 K. The reduced Raman spectra below 250 cm^{-1} are reproduced by a superposition of one relaxation mode and two damped harmonic oscillator modes. The multiple-random-telegraph (MRT) model, which takes into account inertia and memory effects, is applied to analyze the relaxation component. Two damped harmonic oscillators around 50 cm^{-1} and 180 cm^{-1} are known as a bendinglike mode and a stretchinglike mode, respectively. It is found that the intensity of the bendinglike mode in water (heavy water) gradually decreases with increasing temperature, and finally vanishes above about 296 K (306 K). The relaxation time of the MRT model is interpreted as representing the averaged lifetime of the vibrating unit. At high temperature, the relaxation time becomes short, that is to say, the vibrating unit is quickly destroyed before the 50 cm^{-1} mode is oscillating sufficiently. In the present analysis, the strongly disrupted oscillation cannot be distinguished from the relaxation mode which includes the inertia and memory effects. It is found that the low-frequency Raman spectrum of liquid water at high temperature is a good example demonstrating an application of the MRT model. [S1063-651X(99)03608-9]

PACS number(s): 82.20.Fd, 33.20.Fb, 05.40.−a, 82.30.Nr

I. INTRODUCTION

Low-frequency Raman scattering, which occurs in the spectral region below 300 cm^{-1}, has proven to be an effective method for studying molecular dynamics in the liquid state of water. Numerous authors have reported studies on low-frequency Raman scattering [1–4] and depolarized Rayleigh scattering [5–8] of water. Band assignments have been made for two Raman bands in the low-frequency region, a stretching mode and a bending mode, within a system of five water molecules [9–11]. Recently, Raman-induced Kerr effect spectroscopy (RIKES) has been used to investigate the dynamic property of water [12–14].

Many different methods for spectral analysis have been proposed. A Lorentzian function was used to analyze the scattering intensity [5–8,13,15]. Two Lorentzian functions, a narrow central component and a background broad band, were obtained from fitting results. Multimode Brownian oscillators were used to reproduce the whole intensities of RIKES [14]. A Gaussian function was used to interpret the reduced scattering spectra [9,12,16]. Two peaks positioned around 60 cm^{-1} and 190 cm^{-1} were fitted by two Gaussian functions. An Ohmic function was used to fit the central component of the reduced spectra [12]. Reduced spectra at high pressure and high temperature were analyzed by a function based on the relative kinetic energy distribution [11]. Sometimes background has been subtracted during analysis [11,17].

In the present paper, we reexamined the temperature dependence of low-frequency depolarized Raman spectra in liquid water and heavy water. The multiple-random-telegraph (MRT) model [18], which takes into account inertia and memory effects, was applied to analyze the relaxation component. We also discussed the features of the peak around 50 cm^{-1} in the reduced spectra.

II. EXPERIMENT

The samples used were 99.75% D_2O and H_2O which were deionized and distilled. D_2O was purchased from Wako Pure Chemical Industries Co. Ltd., Japan. D_2O and H_2O were filtered through a 0.2 μm millipore filter to remove dust particles and degassed. Then they were introduced into optical cells which were flame sealed.

Depolarized Raman spectra were obtained using a double grating spectrometer (Ramanor U1000, Jobin-Yvon). The exciting light source was an argon ion laser (GLS2165, NEC) operating at 488 nm with power of 500 mW. Right angle scattering geometry was adopted with the (VH) configuration.

Temperature of the sample was controlled with an accuracy within $\pm 0.02\,^{\circ}C$. The temperatures were monitored with Chromel-Constantan thermocouples provided by the Chemical Thermodynamics Laboratory, Osaka University.

All spectra were recorded in the frequency range from -50 cm^{-1} to 250 cm^{-1} at intervals of 0.2 cm^{-1} and in the temperature range from 266 K ($-7\,^{\circ}C$) to 350 K ($77\,^{\circ}C$) at intervals of $4\,^{\circ}C$. We used the spectra from 1.4 cm^{-1} to 250 cm^{-1} for fitting analyses.

III. RESULTS AND ANALYSES

A. Calculation of susceptibility

The dynamic susceptibility $\chi''(\nu)$ is given by

$$\chi''(\nu)=K(\nu_i-\nu)^{-4}[n(\nu)+1]^{-1}I(\nu), \qquad (1)$$

where $I(\nu)$ is the Raman spectral intensity, $n(\nu)=[\exp(hc\nu/kT)-1]^{-1}$ is the Bose-Einstein factor, ν_i is the frequency of incident laser light in cm^{-1}, K is the instrumental constant, T is the absolute temperature, and c is the velocity of light. The variable ν is the Raman frequency shift, also in cm^{-1}.

In the liquid state, we expect three types of contributions for the depolarized Raman susceptibility: intramolecular vibrations, intermolecular motions, and other collective motions. Intramolecular vibrations are observed above about 300 cm^{-1}. Several types of intermolecular motions have been proposed and discussed [19]. For the hydrogen-bonded system, we suppose oscillatory motions as intermolecular motions, because a restoring force would have an effect between hydrogen-bonded molecules.

The Raman intensity corresponding to a single mode is written in the form

$$I(\omega)=\frac{1}{2\pi}\int dt e^{-i\omega t}\langle q(0)q(t)\rangle. \tag{2}$$

Interaction between incident light and electrons is described using the polarizability of electrons α:

$$\alpha(Q)\equiv\left(\frac{d\mu}{d\boldsymbol{E}}\right)_0 \tag{3}$$

$$=\alpha_0+\left(\frac{d\alpha}{dQ}\right)_0 Q+\left(\frac{d^2\alpha}{dQdQ'}\right)_0 QQ'+\cdots. \tag{4}$$

α is modulated by $q(t)$. Finally the Raman spectral intensity is written using the fluctuation-dissipation theorem in the following form:

$$I(\omega)=\left(\frac{k_BT}{\pi\omega}\right)\chi''(\omega). \tag{5}$$

The $q(t)$ is usually supposed as an oscillation mode. We consider that any collective motion which makes the right-hand side of Eq. (2) a nonzero value can contribute to the Raman susceptibility.

We analyze the reduced Raman spectra by using a simple phenomenological model. There are three peaks in the reduced Raman spectra at low temperature and two peaks at high temperature. Each band shape is calculated from Eqs. (2) and (5) by using the time evolution of $q(t)$. So we model an equation of motion for each $q(t)$ under the following postulate: the equation of motion is a second order differential equation of time which contains the terms of inertia, damping, potential, external field, and random forces. In general, the equation of motion of $q(t)$ is a stochastic differential equation such as a Langevin equation and the solution is obtained as the infinite order of a continued fraction using the projection operator method [20]. When this continued fraction was truncated at third order, it has been used as a fitting function to analyze far-infrared absorption [21,22]. However, with the projection operator method, it is difficult to evaluate the truncation error.

The random forces in the equation of motion can be treated as constant when the vibrational motion is much faster than the thermal fluctuations. In this case, the solution of the equation of motion is described as a simple damped harmonic oscillator. On the other hand, when the relevant motions are much slower than thermal fluctuations the inertia term can be neglected. This usually occurs in the very low-frequency region below 1 THz. Then random forces can be treated as a white noise source and the solution of the equation of motion becomes the Debye function. In the intermediate-frequency region, the inertia term cannot be neglected and such correlations as the memory effect in the random forces must be considered. For this, we propose the simple phenomenological model described in the next subsection instead of solving the stochastic differential equation directly.

B. Fitting function

Equivalence between the reduced spectrum of light scattering and the spectrum of far-infrared absorption has already been proven [23]. We apply the dielectric relaxation function of the MRT model which takes into account the inertia and memory effects to analyze the low-frequency depolarized Raman spectra [18].

Generally the complex dielectric function has the form

$$\chi^*(\omega)=1-i\omega v[s], \tag{6}$$

where $s=i\omega$. In this equation, $v[s]$ is given by the following continued fraction for an asymmetric case of the present MRT model:

$$v[s]=\cfrac{1}{s+\cfrac{N\tilde{\Delta}_0^2}{s+\tilde{\gamma}+\cfrac{2(N-1)\tilde{\Delta}_0^2}{s+2\tilde{\gamma}+\cfrac{3(N-2)\tilde{\Delta}_0^2}{s+3\tilde{\gamma}+\cdots\cfrac{}{s+(N-1)\tilde{\gamma}+\cfrac{N\tilde{\Delta}_0^2}{s+N\tilde{\gamma}}}}}}}, \tag{7}$$

where $\tilde{\Delta}_0^2=\Delta_0^2(1-\sigma^2)$ and $\tilde{\gamma}=\gamma-2i\sigma$. The MRT processes are composed of N independent random telegraph processes each of which takes the value $\pm\Delta_0$. The γ is the inverse of the characteristic time of the random telegraph process. A nonzero value of σ means that each probability of the random telegraph processes is asymmetric. This model naturally includes two specific cases: Gaussian-Markovian limit ($N\rightarrow\infty$) and narrowing limit ($\alpha_0\ll 1$). The narrowing limit corresponds to the Debye type relaxation. We use Δ_0, $\alpha_0(=\Delta_0/\gamma)$, σ, N, and relaxation strength A_r as fitting parameters to analyze the depolarized low-frequency Raman spectra.

In addition to the relaxational mode of the central component, two broad peaks are observed below 250 cm^{-1}; around 50 cm^{-1} and 180 cm^{-1}. Two damped harmonic oscillators are used to fit these two bands. The fitting function is given by

$$\chi''(\nu)=A_r\chi_r''(\Delta_0,\alpha_0,\sigma,N;\nu)+A_1\chi_\nu''(\nu_1,g_1;\nu)+A_2\chi_\nu''(\nu_2,g_2;\nu). \tag{8}$$

In the MRT model N means the number of independent random telegraph processes and must be a positive integer. We cannot determine the value of N from the experimental results only. Thus we suppose the simplest case in the present analysis, $N=1$.

In Eq. (8), the relaxation time is not a fitting parameter. To calculate the relaxation time, we define $v(t)$ in the time domain as the inverse Laplace transform of the $v[s]$ given by

$$v(t)=\{\cosh(\tilde{\gamma}t/2\tilde{a})+\tilde{a}\sinh(\tilde{\gamma}t/2\tilde{a})\}^N e^{-N\tilde{\gamma}t/2}, \tag{9}$$

where

$$\tilde{a}=[1-4(\tilde{\Delta}_0/\tilde{\gamma})^2]^{-1/2} \tag{10}$$

and $v(0)=1$. Then we obtain the relaxation time from the following equation:

$$|v(t)|-\frac{1}{2}=0. \tag{11}$$

C. Best-fitted results

Figures 1(a)–1(c) show typical *VH* spectra of liquid water with the best fitted curves. Figures 2(a)–2(c) are the corresponding spectra of heavy water. One relaxation mode and two damped harmonic oscillators around 50 cm^{-1} and 180 cm^{-1} are needed to fit the spectra below room temperature. The MRT model has a broad peak around 50 cm^{-1} at low temperature. Both the bendinglike mode and the stretchinglike mode decrease with increasing temperature. Above room temperature, the bendinglike mode is not necessary to fit the spectra, that is to say, just the MRT model with the stretchinglike mode can reproduce the whole spectra.

Figures 3(a) and 3(b) show the temperature dependencies of mode intensities. The intensity of the MRT mode and bendinglike mode gradually decrease with increasing temperature. The intensity of the bendinglike mode of water and heavy water vanish at 296 K and 306 K, respectively. The intensity of the stretchinglike mode slightly decreases with increasing temperature.

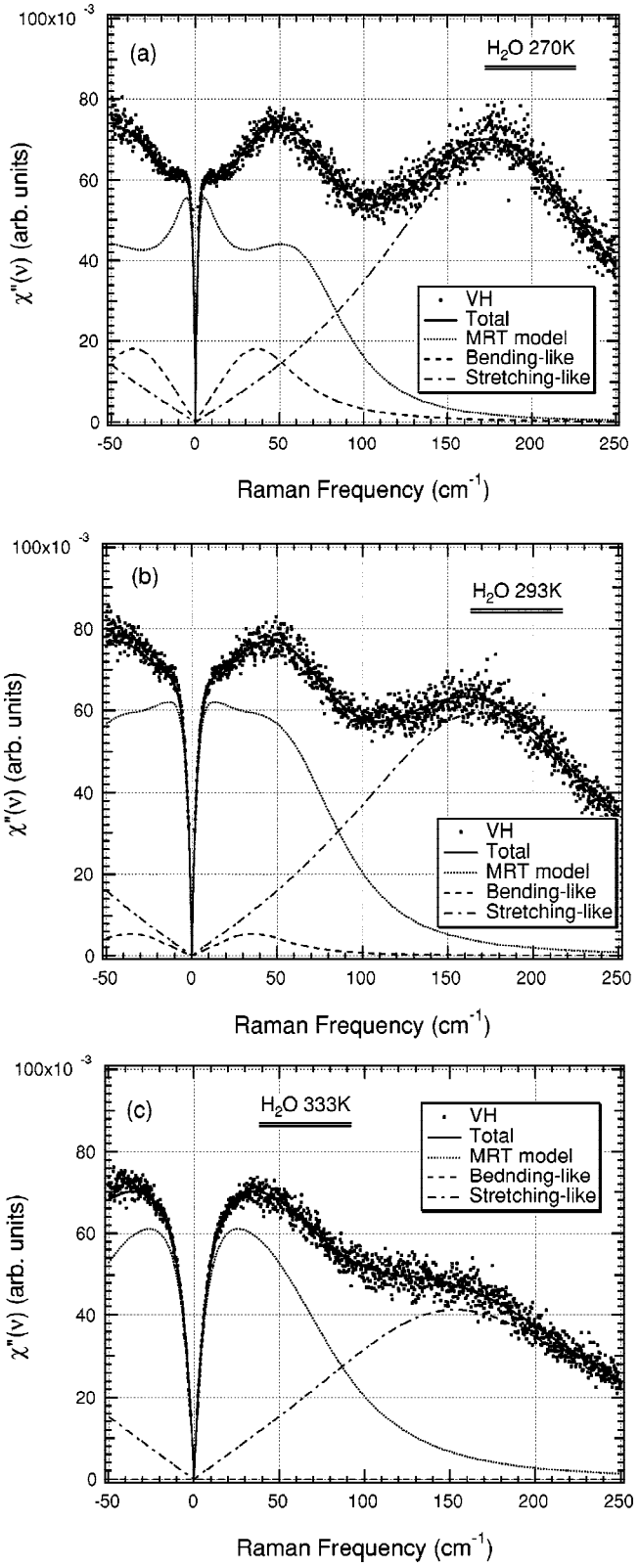

FIG. 1. Reduced low-frequency Raman spectra of water with the best-fitted curves. (a) Supercooled water (270 K), (b) at room temperature (293 K), and (c) at high temperature (333 K).

Figure 4(a) shows the temperature dependencies of the relaxation time of the MRT model. The relaxation time of

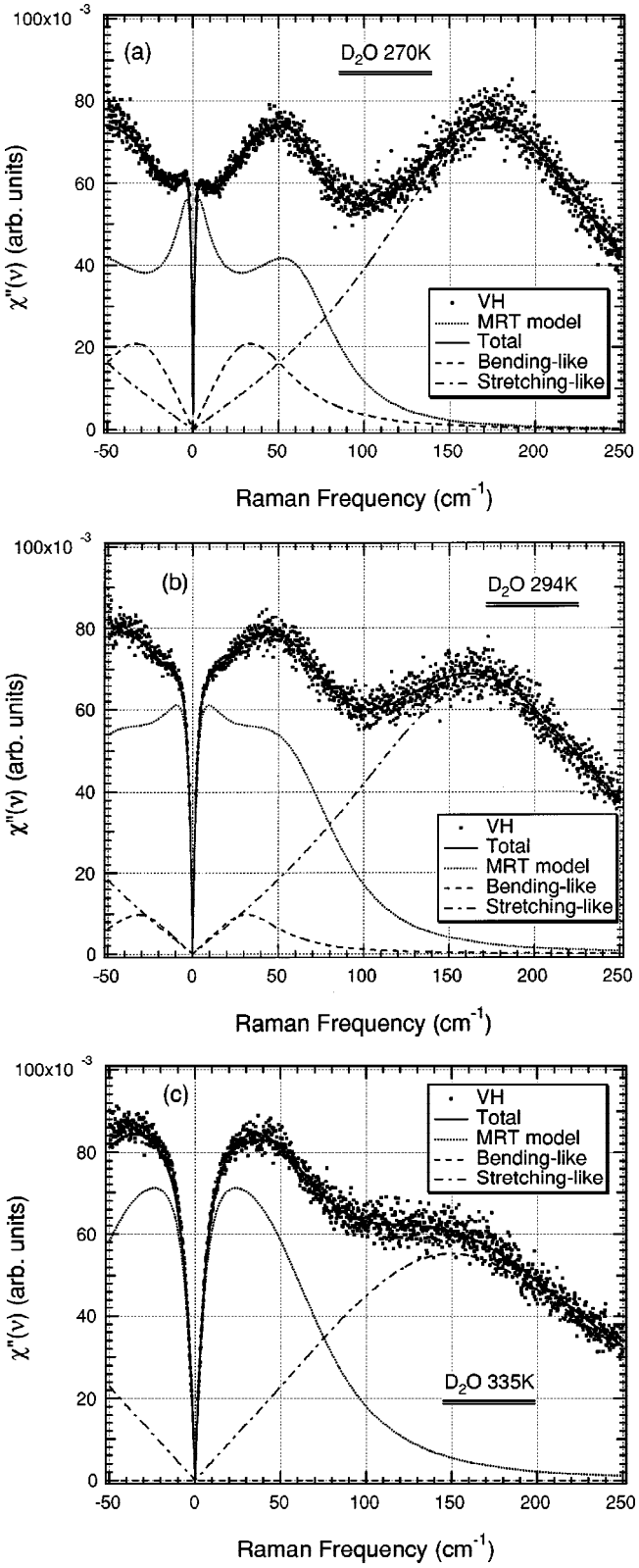

FIG. 2. Reduced low-frequency Raman spectra of heavy water with the best-fitted curves. (a) Supercooled water (270 K), (b) at room temperature (294 K), and (c) at high temperature (335 K).

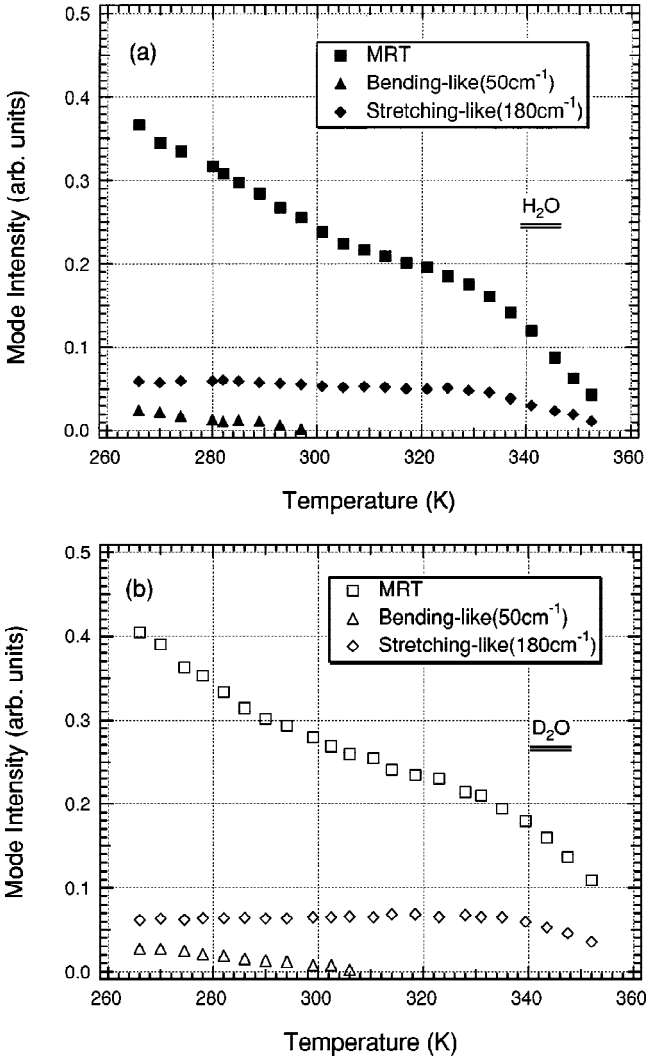

FIG. 3. Temperature dependencies of the intensity of each mode for (a) water and (b) heavy water.

heavy water is always longer than that of water. Figure 4(b) shows the modulation speed of the two-state jump process. Figure 4(c) shows the parameter σ which describes the degree of asymmetry of the two-state jump process. The two-state jump process tends to become symmetric with increasing temperature.

Figures 5(a) and 5(b) show the temperature dependencies of the characteristic frequencies and the damping constants in water and heavy water. The characteristic frequencies of both bendinglike (ν_{50}) and stretchinglike (ν_{180}) modes slightly shift towards the low-frequency side. The damping constant of the stretchinglike mode (g_{180}) increases with increasing temperature, while the damping constant of the bendinglike mode (g_{50}) decreases with increasing temperature. The characteristic frequencies of both the stretchinglike mode and the bendinglike mode are almost the same for water and heavy water.

Figure 6 shows the power spectrum of the two-state jump process corresponding to the best-fit result of water at 293 K. The power spectrum is obtained by joining three spectra which were calculated using a random series in different spectral ranges. The power spectrum of the two-state jump process decreases linearly above 30 cm^{-1}.

IV. DISCUSSION

The central component of the low-frequency depolarized Raman spectra of liquid water and aqueous solutions has

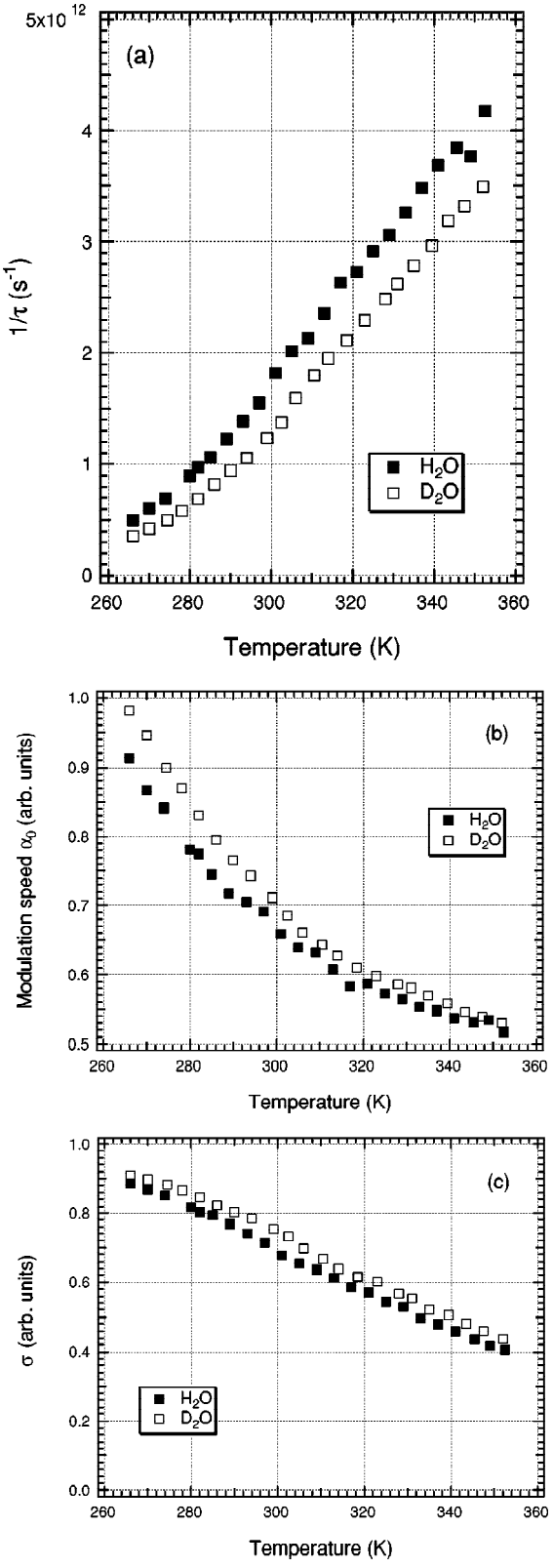

FIG. 4. Temperature dependencies of parameters of the MRT model. (a) Relaxation time and (b) modulation speed of the two-state jump process. (c) σ from Eq. (7).

been analyzed by using the Debye type relaxation function [16] or Cole-Cole type relaxation function which is equivalent to the symmetrically broadened Debye function [24,25]. The Debye function is calculated from the Langevin equa-

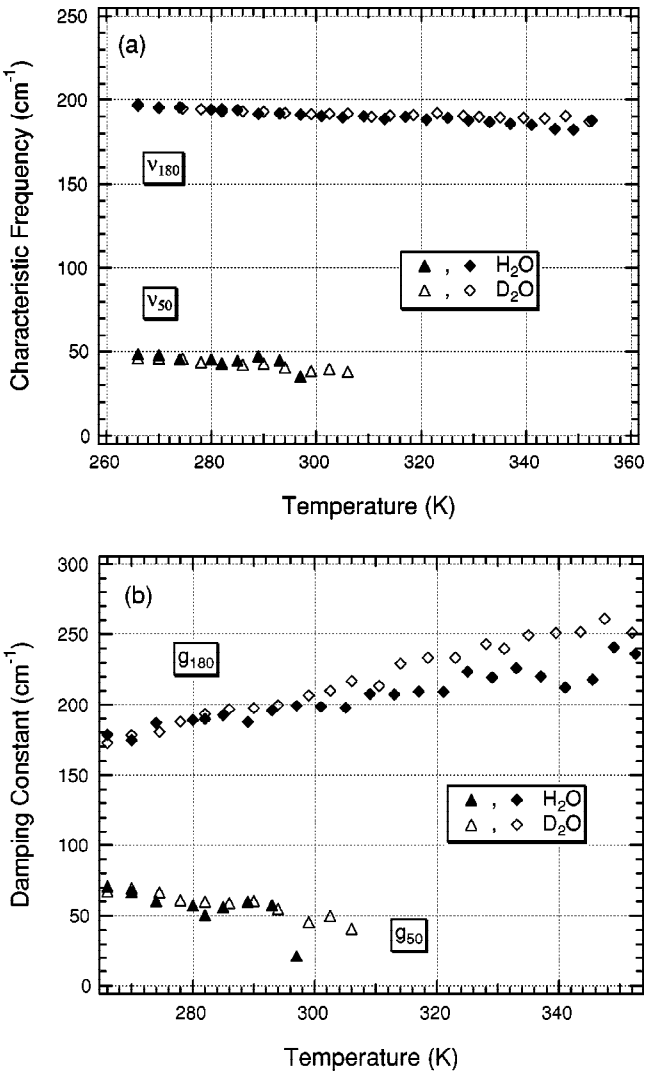

FIG. 5. Temperature dependencies of the parameters of damped harmonic oscillators. (a) Characteristic frequencies and (b) damping constants.

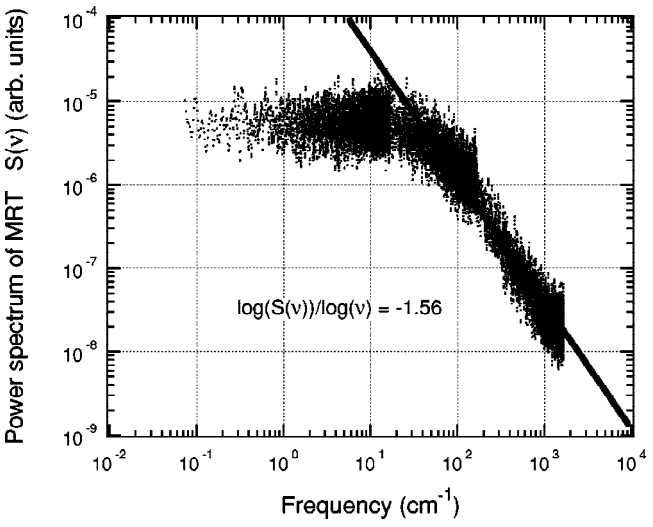

FIG. 6. Power spectrum of the two-state jump process corresponding to the water at 293 K.

tion of a rotating dipole under approximations of overdamped limit and narrowing limit. These approximations are appropriate for frequencies below millimeter wave. As a result of the overdamped approximation, absorption profile of the Debye function reaches a plateau value above about 1 THz (~ 30 cm^{-1}). Therefore the overdamped approximation cannot be applied to analyze the low-frequency Raman spectra above the THz region, i.e., the use of Debye or Cole-Cole functions meets with a fundamental difficulty in this frequency region. Onodera [26] derived a modified Debye function which introduces a cutoff frequency. However, the modified Debye function which is equivalent to the inertia-corrected Debye model is insufficient to fit the relaxation mode in the low-frequency Raman spectra, because it is based on the narrowing limit only. A heat bath should act as a white noise source when the time scales of the fluctuating dipole or polarizability are much slower than the time scale of the fluctuation in the heat bath. In the opposite case, the heat bath can be treated as a slow drift term or a constant term in the equation of motion. When both time scales are of comparable order, the narrowing limit approximation breaks down and the heat bath must be treated as a colored noise source. We propose the use of the relaxation function which includes, as a special case, both the overdamped limit and the narrowing limit to analyze the low-frequency depolarized Raman spectra.

We have considered that the vibration modes observed around 50 cm^{-1} and 180 cm^{-1} correspond, respectively, to a bendinglike mode and a stretchinglike mode of the intermolecular vibration within a system of five water molecules. Walrafen and co-workers have also presented this assignment [9–11]. We think that the low-frequency depolarized Raman scattering selectively detects the intermolecular vibration induced in the vibrating unit of five water molecules embedded in the hydrogen-bond network. The large damping constants of these modes represent the distribution of the characteristic frequencies originating from inhomogeneity of the hydrogen-bond network, and the lifetime of the intermolecular vibration modes should be shorter than that of the intramolecular vibration mode because the ''lattice'' does not in the liquid state. As shown in Fig. 5(a), the characteristic frequencies of the stretchinglike and the bendinglike modes shift to the low-frequency side with increasing temperature. The damping constant of the stretchinglike mode increases with increasing temperature. This temperature dependence of the stretchinglike mode indicates that the intermolecular interaction becomes weak and the lifetime of the vibration becomes short. The temperature dependence of the damping constant of the bendinglike mode behaves differently from that of the stretchinglike mode. The intensity of the bendinglike mode decreases rapidly with increasing temperature, while that of the stretchinglike mode decreases only gradually.

We emphasize that the reduced Raman spectra are fitted well with only a MRT function and a stretchinglike vibration mode above 296 K (306 K for heavy water). The vibrating unit which has a certain spatio and temporal correlation is needed for the intermolecular vibration. We interpret the relaxation time of the MRT model as the averaging lifetime of the vibrating unit. At high temperature, the relaxation time becomes short, that is, the vibrating unit is destroyed quickly before the 50 cm^{-1} mode is oscillating sufficiently. In our analysis, the strongly disrupted oscillation cannot be distinguished from the relaxation mode which includes the inertia and memory effects. The large damping constant of the 180 cm^{-1} mode at high temperature indicates that the lifetime of the mode becomes short due to breakup of the vibrating unit. The 180 cm^{-1} mode can vibrate about 20 times during the lifetime of the vibrating unit, so the intensity of this mode remains at temperatures above 330 K, in contrast to the 50 cm^{-1} mode. Hasted *et al.* [27] have reported that there are two broad absorption peaks at 200 cm^{-1} and 49 cm^{-1}, and significantly the 49 cm^{-1} one disappears at 303 K.

Majolino *et al.* [28] have reported on the connected structure of water. They showed the temperature dependence of a crossover frequency between the phonon and fracton regimes based on the correlated-site percolation model. They noted the crossover frequency is directly connected with the correlation length. The crossover frequency decreased with decreasing temperature, i.e., the correlation length increases with decreasing temperature. Our fitting results indicate that the lifetime of the vibrating unit is longer at low temperature and is shorter at high temperature. However, the structure of the hydrogen-bond network is not explicitly included in our scheme because our model is only based on the stochastic processes and the linear response theory. Therefore our present results are consistent with the results of the phonon-fracton model.

The crossover frequency determined by Majolino *et al.* is identical to the peak frequency of the relaxation mode in our analysis. The localized mode is present above the crossover frequency in terms of the percolating network model. On the other hand, the MRT model gives the Debye type relaxation in the low-frequency tail and gives the oscillationlike spectrum in the high-frequency tail due to the breakdown of the narrowing and overdamped limits. In addition to these spectral responses the ''true'' bendinglike mode is needed in our fitting function at low temperature. Therefore the feature of the density of state changes around the crossover frequency based on the percolation network model and the change of the band shape of the susceptibility due to the inertia and memory effects are different aspects of the same phenomena.

We have demonstrated the application of the MRT model to the Raman spectra of CCl_4, acetone, and chloroform [29]. There is no hydrogen bonding in these liquids and a single peak is observed around 50 cm^{-1}. These spectra are well fitted by one MRT function. On the other hand, both the damped harmonic oscillators and the Debye type relaxation cannot fit these band shapes. We have also found that the parameter α_0, the correlation strength of the heat bath, can be used as an indicator of structure-breaking and structure-making effects of cations in aqueous electrolyte solutions [30]. Breakdown of both the overdamped limit and the narrowing limit of the equation of motion is essential to fit the band shapes. The approximation for the basic equation of motion varies with the time scale of interest. We propose that the model including the inertia and memory effects is applicable not only to a simple molecular liquid, but also network forming complex liquids [31], including liquid water.

The isotope effect between water and heavy water is not observed in the characteristic frequencies of the bendinglike

and stretchinglike modes in the present analysis. The damping constants of the stretchinglike mode in heavy water are larger than those in water above 300 K. As shown in Figs. 3(a) and 3(b), the intensity of the stretchinglike and the bendinglike modes in water decreases more rapidly than that in heavy water with increasing temperature. The intensity of the bendinglike mode in water vanishes at around 296 K and that in heavy water vanishes at the higher temperature, 306 K. The breakup of the hydrogen-bond network causes the decrease of the intensity of vibration modes and the distortion of the hydrogen-bond network causes the increase of the damping constant. The present result is consistent with the fact that the hydrogen-bond energy in heavy water is 5% stronger than that in liquid water [32,33].

In the temperature dependencies of parameters in the MRT model, the isotope effect is clearly observed as noted below. The relaxation time τ, the modulation speed of two-state jump processes α_0, and the parameter for asymmetric distribution σ in water are always smaller than those in heavy water as shown in Figs. 4(a), 4(b), and 4(c), respectively. We consider that the relaxation time τ represents the lifetime of the hydrogen-bond network on a mesoscopic scale. The α_0 represents the degree of time correlation for the fluctuation of individual water molecules. When the microscopic environment around an individual water molecule becomes more inhomogeneous, the values of both α_0 and σ become larger. The τ does not directly include the effect of such an inhomogeneity, because τ is considered as the correlation time of fluctuating polarizability which originates from collective motions of water molecules. The collective dynamics of hydrogen-bonded water molecules is driven by the heat bath which is non-Gaussian and nonwhite, that is to say, the fluctuation of the heat bath has a certain time correlation. The differences of the values of τ, α_0, and σ between water and heavy water as a function of temperature are consistent with the fact that the hydrogen-bond energy in heavy water is stronger than that in water.

As shown in Figs. 1 and 2, intensity of the bendinglike mode is smaller than that of the stretchinglike mode. This relation is the same as seen in the reduced Raman spectra of ice I_h [16,34]. In contrast to the use of the MRT model, the use of the Cole-Cole function leads to the opposite result: intensity of the bendinglike mode is larger than that of the stretchinglike mode.

At room temperature, the Cole-Cole function produces a gradually decreasing background which is about 14% of the total intensity at 250 cm^{-1} [35]. Because of the inertia effect, the MRT model decreases faster than ν^{-1} and does not show significant background above 200 cm^{-1}. Although the behavior between the Cole-Cole function and the MRT model differs, the accuracy of the fit is almost the same. No background subtraction is required for the analysis of the present low-frequency depolarized Raman spectra.

Another candidate to model the relaxation mode in the Raman spectra is the itinerant oscillator (IO) which was applied to calculate the Debye and far-infrared (Poley) absorption spectra of dipolar liquids [36,37]. The parametric form of polarizability based on the IO is described in [38]. The IO also incorporates the inertia effect and can produce a harmonic peak. There are six free parameters in the parametric form of IO. The IO model can fit the band shape of the MRT model in the best-fitted results for water qualitatively. Harmonic peaks in the IO model tend to separate from the main relaxation peak. On the other hand, the harmonic shoulder in the MRT model is included in the main relaxation peak well. Thus these models show similar, but somewhat different band shapes. Detailed discussions on the similarity and the difference between the above two models will be a future research problem.

Figure 6 shows the power spectrum of the two-state jump process for liquid water at 293 K. We calculated the spectrum by using a random number series. From Fig. 6 we can see that there is a certain correlation in the heat bath. Time sequences and power spectrum of the fluctuation of the total system energy have been calculated in liquid water [39]. Time sequences of the variation of the local structure have also been calculated [40]. From these papers we can easily see that a certain correlation of fluctuations does exist. Although Fig. 6 shows the power spectrum of the fluctuation which acts on the collective relaxational motion only, our results are valuable for comparison with the above molecular dynamics calculations.

V. CONCLUDING REMARKS

We have measured low-frequency depolarized Raman spectra of liquid water and heavy water from 266 K to 350 K. The reduced Raman spectra were well fitted by the superposition of one MRT function as a relaxation mode and the two damped harmonic oscillator modes. The MRT model took into account the inertia and memory effects. The isotope effect appeared in the fitting parameters of the MRT model τ, α_0, and σ. The characteristic frequencies of both the stretchinglike mode and the bendinglike modes shifted toward the low-frequency side with increasing temperature. The intensity of the bendinglike mode was always smaller than that of the stretchinglike mode. No background correction was necessary for spectral analysis. The intensity of the bendinglike mode in water (heavy water) gradually decreased with increasing temperature, and finally vanished above about 296 K (306 K). Our results were consistent with the far-infrared absorption spectral features. At high temperature, the bendinglike mode was strongly disrupted and could not be distinguished from the relaxation band shape which takes into account the inertia and memory effects. The MRT model could well characterize the features in the relaxation component of low-frequency Raman spectra.

ACKNOWLEDGMENTS

We would like to thank Professor F. Shibata for many discussions and valuable advice. This work was partially supported by a Grant-in-Aid for Scientific Research from the Ministry of Education, Science, Culture, and Sports.

[1] M. H. Brooker and M. Perrot, J. Chem. Phys. **74**, 2795 (1981).
[2] O. F. Nielsen and D. H. Christensen, J. Chem. Phys. **82**, 1183 (1985).
[3] O. F. Nielsen, J. Raman Spectrosc. **20**, 221 (1989).
[4] M. A. Ricci, G. Signorelli, and V. Mazzacurati, J. Phys.: Condens. Matter **2**, SA183 (1990).
[5] C. J. Montrose, J. A. Bucaro, J. Marshall-Coakley, and T. A. Litovitz, J. Chem. Phys. **60**, 5025 (1974).
[6] O. Conde and J. Teixeira, J. Phys. (France) **44**, 523 (1983).
[7] O. Conde and J. Teixeira, Mol. Phys. **53**, 951 (1984).
[8] F. Aliotta, C. Vasi, G. Maisano, D. Majolino, F. Mallamace, and P. Migliardo, J. Chem. Phys. **84**, 4731 (1986).
[9] G. E. Walrafen, M. R. Fisher, M. S. Hokmabadi, and W.-H. Yang, J. Chem. Phys. **85**, 6970 (1986).
[10] G. W. Walrafen, J. Phys. Chem. **94**, 2237 (1990).
[11] G. E. Walrafen, Y. C. Chu, and G. J. Piermarini, J. Phys. Chem. **100**, 10 363 (1996).
[12] Y. J. Chang and J. Edward W. Castner, J. Chem. Phys. **99**, 7289 (1993).
[13] E. W. Castner, Jr., Y. J. Chang, Y. C. Chu, and G. E. Walrafen, J. Chem. Phys. **102**, 653 (1995).
[14] S. Palese, S. Mukamel, R. J. D. Miller, and W. T. Lotshaw, J. Phys. Chem. **100**, 10 380 (1996).
[15] V. Mazzacurati, A. Nucara, M. A. Ricci, G. Ruocco, and G. Signorelli, J. Chem. Phys. **93**, 7767 (1990).
[16] K. Mizoguchi, Y. Hori, and Y. Tominaga, J. Chem. Phys. **97**, 1961 (1992).
[17] G. E. Walrafen, M. S. Hokmabadi, W.-H. Yang, Y. C. Chu, and B. Monosmith, J. Phys. Chem. **93**, 2909 (1989).
[18] F. Shibata, C. Uchiyama, and K. Maruyama, Physica A **161**, 42 (1989).
[19] R. Shuker and R. W. Gammon, J. Chem. Phys. **35**, 4784 (1971).
[20] N. G. V. Kampen, *Stochastic Processes in Physics and Chemistry* (Elsevier, Amsterdam, 1992).
[21] W. Coffey, Adv. Chem. Phys. **63**, 69 (1985).
[22] B. N. Flanders, R. A. Cheville, D. Grischkowsky, and N. F. Scherer, J. Phys. Chem. **100**, 11 824 (1996).
[23] B. M. Abdrakhmanov, A. I. Burshtein, and S. I. Temkin, Chem. Phys. **143**, 297 (1990).
[24] Y. Wang and Y. Tominaga, J. Chem. Phys. **101**, 3453 (1994).
[25] Y. Wang and Y. Tominaga, J. Chem. Phys. **104**, 1 (1996).
[26] Y. Onodera, J. Phys. Soc. Jpn. **62**, 4104 (1993).
[27] J. B. Hasted, S. K. Husain, F. A. M. Frescura, and J. R. Birch, Chem. Phys. Lett. **118**, 622 (1985).
[28] D. Majolino, F. Mallamace, P. Migliardo, F. Aliotta, N. Micali, and C. Vasi, Phys. Rev. E **47**, 2669 (1993).
[29] Y. Amo and Y. Tominaga, J. Chem. Phys. **109**, 3994 (1998).
[30] Y. Amo and Y. Tominaga, Phys. Rev. E **58**, 7553 (1998).
[31] Y. Amo and Y. Tominaga, Physica A **265**, 410 (1999).
[32] G. Nemethy and H. A. Scheraga, J. Chem. Phys. **41**, 680 (1964).
[33] A. I. Kudish and D. Wolf, J. Phys. Chem. **79**, 272 (1975).
[34] S. Krishnamurthy, R. Bansil, and J. Wiafe-Akenten, J. Chem. Phys. **79**, 5863 (1983).
[35] Y. Tominaga, Y. Wang, A. Fujiwara, and K. Mizoguchi, J. Mol. Liq. **65/66**, 187 (1995).
[36] W. Coffey, M. Evans, and P. Gligolini, *Molecular Diffusion and Spectra* (Wiley, New York, 1984).
[37] M. Evans, G. H. Evans, W. T. Coffey, and P. Grigolini, *Molecular Dynamics and Theory of Broad Band Spectroscopy* (Wiley, New York, 1982).
[38] W. T. Coffey, Y. P. Kalmykov, and J. T. Waldron, *The Langevin Equation with Applications in Physics, Chemistry and Electrical Engineering* (World Scientific, Singapore, 1996).
[39] I. Ohmine, J. Phys. Chem. **99**, 6767 (1995).
[40] E. Shiratani and M. Sasai, J. Chem. Phys. **104**, 7671 (1996).